# GPR Surveys and Excavation Ground-Truthing at the San Tau Backbeach Site, Hong Kong

Mick Atha
The Chinese University of Hong Kong
Shatin, NT, Hong Kong
mickatha@cuhk.edu.hk

Wallace Lai and Ray Chang
Department of Land Surveying and Geo-informatics,
The Hong Kong Polytechnic University
Hung Hom, Kowloon, Hong Kong
ray.chang@polyu.edu.hk; wllai@polyu.edu.hk

***Abstract*— This paper presents the results of an archaeological fieldwork project conducted by a pro-geophysics archaeologist (Atha) and two 'archaeo-curious' GPR specialists (Chang and Lai) at the San Tau backbeach site in Hong Kong. Previous small-scale test pitting suggested that the site might be a locally unique Tang dynasty cemetery, with probable later (Northern Song) activity, but grave definition was problematic and the cemetery's wider extent remained unknown. However, the fine-grained, relatively homogenous background appeared ideal for GPR. A two-stage approach was used: a 400MHz antenna was applied in an initial prospection survey, while both 400MHz and 900MHz were used in a second campaign of higher-resolution intra-site analytical survey. The GPR results identified many 'targets' and proved decisive in locating and discriminating both Tang dynasty graves and overlying Northern Song pits. Based on the results of GPR surveys and excavation ground-truthing, it seems the site may in total contain several hundred Tang burials, significant among which were several co-aligned 'warrior burials' with iron weapons and tools. Reference to site records of object types (metallic or non-metallic) and sizes shows that the very different slice images by 400MHz and 900MHz GPR are best explained by the radar footprints in First Fresnel zone (FFZ), which is a function of object depth, antenna frequency, GPR wave velocity in soil, and two-way travel time of the objects' reflections. The findings indicate that GPR is in general highly effective on sandy coastal sites, and in particular can provide useful estimates of the size and character of buried archaeological features and artefacts. Based on our findings, more routine application in local archaeology is therefore strongly recommended.**

***Index Terms*—First Fresnel Zone, Intra-site Analysis, Archaeological Ground-truthing, Tang Cemetery, Sandy Backbeach Sites.**

## I. Introduction

In contrast to Europe, America, and other parts of Southeast Asia [1], where geophysical surveys are a routinely used first stage evaluation tool in both development-funded and research-focused archaeological projects, archaeological geophysics in Hong Kong is very much in its infancy. The project reported upon here was an initial attempt to evaluate the potential of geophysics—in this case GPR—in Hong Kong's richest and most widespread category of archaeological sites: sandy backbeaches.

Our focus was the backbeach site at San Tau on the north coast of Lantau Island, where earlier small-scale excavations suggested the existence of a regionally unique Tang dynasty cemetery. The sandy homogenous background seemed ideal for GPR survey, which it was hoped might help clarify and define subsurface remains, while also enhancing understanding for future site management. Firstly, by revealing the fuller extent of the cemetery; secondly, through identifying 'targets' for further 'ground-truthing' excavations; and lastly, as a tool in intra-site analysis and site characterization. Below we report on the second, higher resolution, campaign of GPR survey and excavation ground-truthing, which was carried out in November-December 2012.

We begin by offering a brief background to the site, then move on to outline the methodology used, present some comparative discussion of the archaeological and GPR results—with a particular emphasis on the interpretive significance of First Fresnel zone data—and finally draw some conclusions.

## II. Background

### *A. Geology & Setting*

The San Tau backbeach lies on the northern edge of a large alluvial fan at the mouth of a short, steep-gradient northeast-facing valley. The backbeach formed in antiquity through storm action [2], and was therefore probably a low, rounded sand dune-like formation in the Tang dynasty. More recent activities of Qing-modern farmers then created the present flat-topped backbeach profile. While the backbeach itself consists entirely of fine sand grading to coarser sand at depth, it overlies clayey debris flow deposits at the foot of the steep granite hill that overlooks the site to the west. While clay-rich sediment can be problematic for GPR, at San Tau it forms the natural substrate over which, from west to east, there is an estimated 1.5m to 3m of sandy backbeach deposits, within which the upper 1m has cultural remains.

### *B. Previous Archaeological Discoveries*

The archaeological potential of the San Tau backbeach site was first recognized in 1997 when a planning-stage feasibility study included the excavation of several shovel tests and test pits [3]. Song and Tang dynasty deposits were

identified, including a Tang storage jar associated with 62 *Kaiyuan Tongbao* copper alloy coins, which prompted a tentative 'cemetery' interpretation. Soon afterwards, during the Second Territory-wide Survey, a 2m x 3m test pit identified two "early Tang" burials supposedly both aligned north-south [4]. Typically for local backbeach sites, no human bone survived and the grave pits—cut into and backfilled with sand—were evidently extremely difficult to define.

Similar problems of definition occurred during our first season of fieldwork, during which, following an initial GPR prospection survey (400MHz, 1 m x 1 m resolution, and 475 $m^2$), targeted excavation revealed intercutting Qing, Northern Song, and Tang features, including seven fully-excavated Tang graves laid out using three different orientations [5].

The 400MHz antenna successfully picked up larger iron artefacts and denser clusters of ceramics and stones, but had, however, failed to highlight pits and graves with fewer and less dense concentrations of grave goods. The homogeneity of sandy sediments within the site meant that no features could be delineated solely on the basis of contrast between fill and site background. The discrimination of feature inclusions—primarily stones and grave goods—was therefore crucially important to the interpretation of GPR targets in terms of cultural activity. In order to enhance our ability in that regard, the use of a more sensitive, higher frequency antenna—in our case 900MHz—was therefore indicated. Depth penetration was not an issue as the results of our first season of fieldwork showed that the bases of Tang graves were typically less than 1m below the modern surface.

*C. Archaeological prospecting by GPR*

Even when an object is within the detectable range of a particular GPR system and the host soil is clutter-free, it does not necessarily mean that it can be imaged. What can and what cannot be imaged depends on two factors: namely vertical dielectric contrast and horizontal resolution. First, a reflecting horizon varies vertically according to dielectric contrast across the vertical interface as a measure of reflection coefficient. Larger contrast increases the signal to noise ratio and is therefore easier to be imaged, as is the case with iron objects buried in non-magnetic sand. Second, horizontal (or spatial) resolution refers to the ability to resolve the lateral changes among reflectors. In this case, the reflected energy reaching the receiving antenna is not from a single point of incidence, but from a circular subsurface downward zone on the reflector (Fig.1), and is known as the First Fresnel Zone (FFZ).

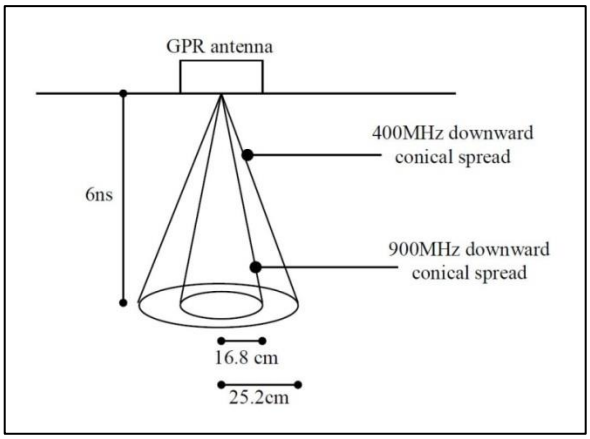

Fig. 1. First Fresnel Zone of 400MHz and 900MHz GPR antennas

FFZ is dependent on time/depth, wave velocity, and frequency. If $t_r$ is the two-way time of a reflector, $f_c$ the frequency of a radar wave, and v the velocity, the FFZ radius F from which most energy comes, is given by:

$$F = 0.5\, v \sqrt{\frac{t_r}{f_c}} \quad \ldots\ldots(1)$$

Object shape can only be accurately imaged if the area of a reflector is larger than the area of the circular zone/radar footprint with radius 'F'. However, if the coverage of the reflector is smaller, diffraction patterns from the edges of the reflector weaken the reflection strength and thus, the clarity of images. From Equation 1, it is important to note that the footprint increases but spatial resolution decreases as a function of depth (i.e. with the increase of time).

For example, for a GPR wave velocity of 0.13 m/ns and if 400MHz GPR is used, the calculated spatial resolution of a reflector is about 25.2 cm (or circular area 1995 $cm^2$) at a time $t_r$ = 6 ns. This means that in theory, the object can be imaged if the reflector is larger than 1995 $cm^2$. In practice, the reported spatial resolution is normally better. Cook [1975] discusses an effective Fresnel zone as equal to half the size of the FFZ, which implies an object with radius 12.6 cm and associated area of 498 $cm^2$ can be imaged if the conditions in the above case are fulfilled [6]. Furthermore, if the size of the object is equal to one-fourth of the FFZ, its reflected amplitude decreases only by 40%, which can be still imaged under favourable conditions.

## III. Methodology

*A. GPR Data Acquisition*

For the second season of fieldwork a higher resolution (0.5 m x 0.5 m and 200 $m^2$) survey was conducted using a GSSI SIR-20 GPR unit and 900MHz antenna, with a 400MHz antenna being also deployed for comparative purposes (Fig.2). The survey was carried out in an orthogonal grid with traverses spaced 0.5 m apart.

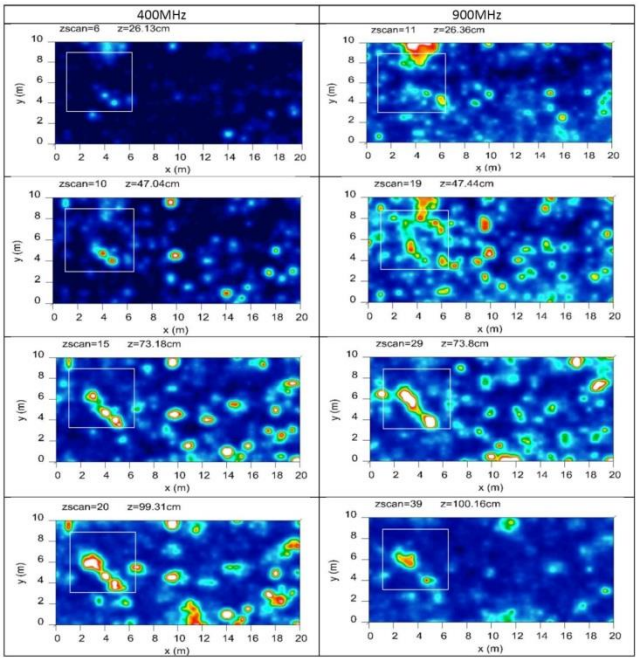


Fig. 2. Time-slice images of 400MHz and 900MHz data with trench outline superimposed (in white)

### *B. Excavation*

A 5m by 5m trench was opened up over a clustering of GPR targets at the western end of the detailed survey area. With the topsoil removed, a series of intercutting pit-like features was identified, and the area was expanded to the north and east in order to expose the full outline in plan of as many features as possible, which eventually created a trench measuring 6m by 5.5m in extent.

The apparent complexity of intercutting features argued against the retention of vertical baulks within the trench. All features were therefore defined and stratigraphic relationships were determined in plan, features were placed into phases, and then smaller pits were half-sectioned and recorded, while potential graves were excavated in plan to allow recording of relative arrangements of grave goods.

## IV. Results

### *A. Overview of Excavation Results*

The excavations identified many pits evidencing three distinct periods/types of activity, in order of deposition: three definite (G17, G18 & G19) and one possible (G20) Tang dynasty graves (on two alignments) (Fig.3); an intense phase of Northern Song pit digging, including pit P28 with frequent burnt stone and fired clay kiln debris and P29 packed with large rounded cobbles; and a number of smaller Qing-early modern pits among which was a stone-packed post-hole (P11) (Fig.4).

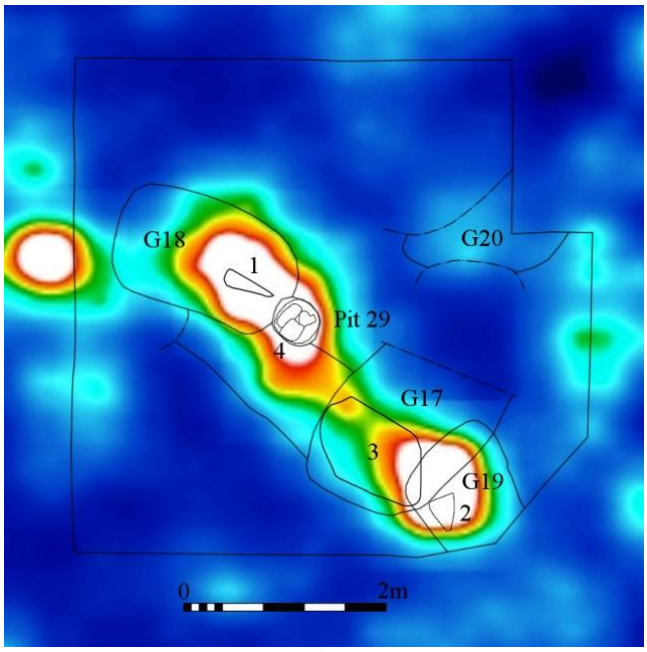


Fig. 3. 900MHz time-slice image for 73.8cm depth with feature/object overlay

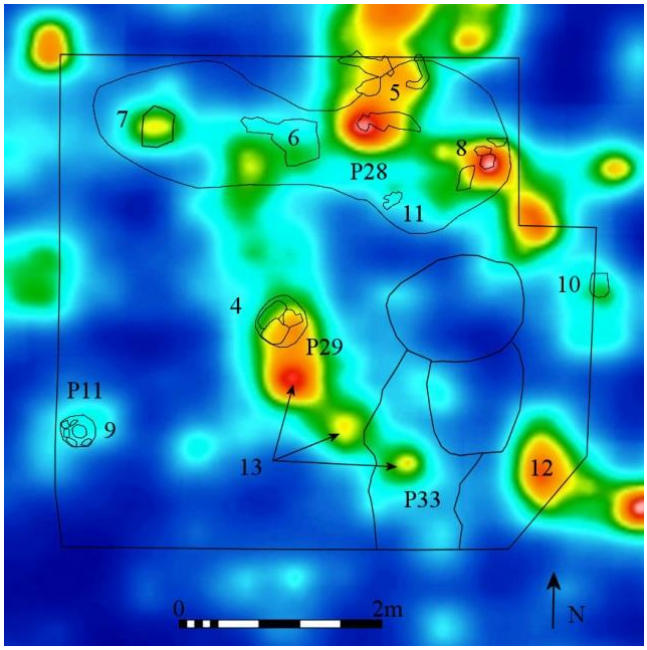


Fig. 4. 900MHz time-slice image at 47.44cm depth with feature/object overlay

### *B. Comparison of 400MHz and 900MHz Responses to Archaeological Features/Artefacts*

Table 1 presents a summary of the main categories (A, B and C) of features and artefacts that produced a response in the 400MHz and 900MHz surveys. According to Equation 1 and previous discussion, the established criteria for best-image are that the ratio of object area to FFZ—hereafter referred to as the 'ratio'—is equal to or larger than unity. For an object with a ratio smaller than unity, its imageability is dependent on whether there is a significant

dielectric contrast across the interface between the host sand and the object. A large contrast can compensate for the negative effect of a ratio < 1 and make small objects still imageable, for example iron grave goods under category A.

TABLE 1: FEATURE/OBJECT CHARACTERISTICS RELATIVE TO FIRST FRESNEL ZONE AREA FOR 400MHZ AND 900MHZ ANTENNAS

| | | | | | | 400MHz GPR | | 900MHz GPR | |
|---|---|---|---|---|---|---|---|---|---|
| Cat. | No. | Archaeological feature/object description | Feature/ object dimensions | Feature/ object area (m2) | Depth (m) | FFZ area at target depth (m2) | Ratio of feature/ object area to FFZ area | FFZ area at target depth m2) | Ratio of feature/ object area to FFZ area |
| A | 1 | Grave G18: iron knife & long iron cleaver | 15cm x 65cm | 0.098 | 0.73 | 0.287 | **0.340** | 0.127 | **0.765** |
| | 2 | Grave G19: small & large iron knives & iron adze-head | 23cm x 29cm | 0.067 | 0.57 | 0.224 | **0.298** | 0.099 | **0.670** |
| B | 3 | Grave G17: pottery, stones, kiln debris & non-ferrous objects | 50cm x 70cm | 0.350 | 0.5 | 0.196 | **1.783** | 0.087 | **4.011** |
| | 4 | Pit P29: densely packed with rounded cobbles | 50cm diam. | 0.196 | 0.55 | 0.216 | **0.907** | 0.096 | **2.042** |
| | 5 | Pit P28: spread of burnt stone & kiln debris | 90cm x 95cm | 0.855 | 0.35 | 0.137 | **6.221** | 0.061 | **13.997** |
| | 6 | Pit P28: spread of burnt stone & kiln debris | 55cm x 83cm | 0.457 | 0.37 | 0.145 | **3.145** | 0.065 | **7.077** |
| | 7 | Pit P28: spread of burnt stone & kiln debris | 35cm x 50cm | 0.175 | 0.37 | 0.145 | **1.204** | 0.065 | **2.710** |
| | 8 | Pit P28: pot, kiln debris & two burnt stones | 30cm x 80cm | 0.240 | 0.37 | 0.145 | **1.652** | 0.065 | **3.716** |
| C | 9 | Pit P11: stone-packed post-pit | 35cm diam. | 0.096 | 0.47 | 0.185 | **0.521** | 0.082 | **1.173** |
| | 10 | Layer 550: pottery cluster | 22cm x 25cm | 0.055 | 0.35 | 0.137 | **0.400** | 0.061 | **0.900** |
| | 11 | Pit P28: spread of burnt stone & kiln debris | 28cm x 30cm | 0.084 | 0.37 | 0.145 | **0.578** | 0.065 | **1.301** |
| | 12 | Layer 550: large stone | 25cm x 35cm | 0.088 | 0.3 | 0.118 | **0.747** | 0.052 | **1.681** |
| | 13 | Layer 514-5: stones & kiln debris? | Up to 15cm x 25cm | 0.038 | 0.4 | 0.157 | **0.242** | 0.070 | **0.544** |

*Category A (Metallic objects, size varies at grave G18 & G19, ratio < 1):*

As Fig.2 attests, graves with large, well-preserved iron weapons and tools produced strong reflections with both antennas. The large bladed weapons in graves G18 and G19 were respectively 40cm and 34cm long (Fig.3 Nos. 1 & 2 respectively) and formed part of clusters of grave goods including other, smaller iron objects, which in the former case were also associated with pottery and stones. Interestingly, as was noted in the first season's prospection-level survey, the long axis of GPR anomalies in time-slice data recorded the orientation of large bladed weapons in the ground, which also reflected the orientation of the graves themselves.

Although in both cases the ratio of object coverage to FFZ was <1 for both antennas, the two grave goods clusters were clearly imageable as the iron offered a strong dielectric contrast with the site background.

*Category B (Non-metallic features/objects with size large enough to intercept radar footprint at grave G17, pit P28, and pit P29, ratio > 1)*

*Mixed Grave Goods Assemblage (G17)*

In contrast to the 'warrior burials' above, grave G17 contained only a small fragment of a double-edged iron sword blade, but included the remains of 11 pottery vessels, two stacks of 6 copper alloy coins, two chunks of kiln debris, and various small silver ingot off-cuts, which formed a fairly dense spread at the south-western end of the grave associated with two stones (Fig.3 No.3).

In this case, the two antennas (Fig.2) seem to have picked up the two stones (c.35cm x 20cm overall) within the larger clustering of pottery grave goods, non-ferrous items, and kiln debris covering around 1.8 times (400MHz) and 4 times (900MHz) FFZ. Why the 400MHz produced a stronger reflection than the 900MHz in this case is unclear, but it did. NB: an attempt to compare the energy levels from the two frequencies is beyond the scope of this paper as it involves a lot other factors like algorithm of normalization and how thick the slices are.

*Stone-Filled Pit P29*

Stone-filled pit P29 measured c.50cm diameter by 40cm deep and was filled with 9 closely set stones in 2-3 layers (Figs. 3 & 4, No.4). The stones ranged in size from 9cm by 10cm by 18cm to 17cm by 18cm by 36cm.

In the case of P29, its small size (ratio 0.907 of 400MHz FFZ area) rather restricted its imageability by that antenna, but in contrast it was clearly defined in the 900MHz data where the ratio was 2.042.

*Spreads of Kiln Debris and Burnt Stones in Pit P28*

In Fig.3 pit P28 contains five spreads of fire-cracked stone and kiln debris (Nos.5-8 & 11), although No.11, being small, is discussed under Category 'C' below. The larger four can be split into two groups of two based on their composition (relative number and size of materials). While all had areas of FFZ >1, spread Nos. 5 and 8 comprised fewer but larger objects (especially larger stones > 0.05m$^2$), whereas spread Nos. 6 and 7 comprised many smaller fragments of stone and kilns debris (each typically < 0.01m$^2$).

In the 900MHz data this resulted in much stronger reflections for Nos. 5 and 8, and much weaker—but still imageable—responses for Nos. 6 and 7. This can be explained in terms of interference, which was limited at Nos.5 and 8, but significantly greater at Nos. 6 and 7. Such factors meant that only No.5—with the largest overall area and least interference—was clearly imageable in the 400MHz data.

All Category B items had poor dielectric contrast compared to the host soil environment, so the key factors governing their relative imageability by the two antennas were overall feature size and interference. Depth is also a key factor as is shown in Fig.2 by the z=26cm time-slice

data. A wide scattering of near-surface stone and kiln debris recorded during excavation is clearly imaged by the 900MHz antenna, but is almost entirely missed by the 400MHz antenna.

*Category C (Non-metallic features/objects with size, too small to intercept radar footprint at pit P11, pit P28, layer 550 and layer 514-5, ratio < 1):*

*Stone-packed Post-hole (P11)*

Stone-packed post-hole P11 measured 35cm diameter by 45cm deep and contained 15 small stones (Fig.4 No.9). At its base was a central 'pad-stone' (12cm x 15cm) surrounded by smaller packing stones, while a further ring of small packing stones was noted near the top of the feature.

The basal stones of P11 produced a clear but weak reflection in the 900MHz data, which also just picked up the surface packing stones, whereas only the deeper stones were barely imageable by the 400MHz antenna

*Layer 550 Pottery Cluster*

A cluster of three pottery vessels, one cup (8cm diameter) and two large fragments of a bowl (20cm diameter) and storage jar (24cm diameter) were seemingly imageable by the 900MHz but not the 400MHz antenna (Fig.4 No.10).

The apparent ability of the 900MHz antenna to even faintly image a pottery cluster of such small area and at such a shallow depth is noteworthy, in particular when the 400MHz showed nothing.

*Small Spread of Kiln Debris & Burnt Stone (P28)*

Even the smallest spread of stone and kiln debris in P28 (Fig.4 No.11) was faintly imageable in the 900MHz data, but again was missed by the 400MHz antenna.

*Individual Large Stones & Kiln Debris*

In Fig.4, No.12 and the northernmost of the three reflectors arrowed No.13 are perhaps both the result of large stones (>25cm long) noted in those areas. However, why the latter produced a strong response while No.12 was not imaged by the 400MHz antenna is a mystery. The two smaller 'moderate' reflections also labelled '13' are similarly perplexing as they are imaged by both antennas weakly in the z=26cm time-slice and more strongly in the z=47cm plot. The southeasternmost seems to coincide with a chunk of kiln debris in pit P33 (10cm by 12cm), but something this small should not really be imageable, in particular by the 400MHz antenna. The central reflector labelled '13' may have resulted from one or more large stones recorded between P29 and P33 during excavation.

Category 'C' objects all had poor dielectric contrast and for the 400MHz antenna a ratio of object area to FFZ of <1 and some were therefore not imageable, while others, quite surprisingly, were. Overall, though, the 900MHz antenna is clearly far more effective than the 400MHz at identifying and defining archaeological remains of this type.

## V. CONCLUSIONS

This comparative study of the results of two different GPR antennas and archaeological ground-truthing offers an initial insight into the technique's effectiveness in Hong Kong backbeach conditions. A number of important findings can be highlighted.

In general, it can be said that the use of a 400MHz antenna—the 'standard' equipment used in archaeological GPR work—is effective in picking up large iron objects (G18 & G19) and features containing relatively dense clusters of artefacts and stones (G17 & P29).

All the above remains were clearly defined by the 900MHz antenna, which was also far more effective at discriminating objects and features comprising smaller and less-dense/conductive archaeological remains, in particular scatters of burnt stone and kiln debris lying within the uppermost 30cms of the site sequence. This is important, as many backbeach sites in Hong Kong—probably as a result of Qing-early modern agricultural truncation-flattening—can have quite ancient archaeological deposits surviving just beneath the surface. Moreover, early historical kilns and associated debris have been recorded in almost every backbeach excavation so far conducted in the territory, so the 900MHz antenna's ability to discriminate such material is very encouraging.

In addition, although not identified at San Tau, prehistoric activity—evidenced elsewhere mainly by spreads and clusters of pottery and stones—is widely encountered on local backbeach sites and would respond well to GPR. Where sites are deep a 400MHz antenna may be needed [7], which will reduce the range of what might be imageable, but is still surely better than relying on the limited coverage and partial site evaluations presently provided by a few auger drills and test pits.

Last but not least, it is important to remember that although many of the stones identified by GPR and excavation at San Tau were, strictly speaking, neither artefacts nor structures, backbeaches are primarily natural accumulations of sand, so any larger stones or stone clusters identified invariably indicate loci of historical or prehistoric human activity. The ability of GPR to identify the position and depth of such loci in 3-D thus offers a powerful predictive tool for use in future archaeological investigations of backbeach sites, as well as other sites on sandy coastal alluvium such as that encountered at To Kwa Wan, Kowloon Bay.

The latter site has of late been much in the news in Hong Kong because archaeologically important structural remains discovered during rescue excavations led to huge delays and cost overruns in a major infrastructural project. As the San Tau project has shown, GPR should have had little trouble highlighting the presence of major structures within the sandy sediment of the To Kwa Wan site. In many other parts of the world, geophysical survey is a routinely used

first stage evaluation tool in development-funded archaeological investigations, and the time now seems ripe for Hong Kong to 'join the party'.

## ACKNOWLEDGMENT

Mick Atha thanks his site supervisors Kennis Yip and Kathy Chan, the Hong Kong Archaeological Society for their kind commission, and the Leisure and Cultural Services Department of the Hong Kong Government for sponsoring the fieldwork.

## REFERENCES

[1] See examples in: L.B. Conyers, Ground penetrating radar for archaeology. AltaMira: Walnut Creek, CA; C.F. Gaffney and J.A. Gater, Revealing the buried past: geophysics for archaeologists. Stroud, Tempus; L.T. Tong, K.H. Lee, C.K. Yeh, Y.T. Huang and C.Y. Liu, "Ground-penetrating radar prospecting in the Peinan Archaeological Site, Taiwan", Terr. Atmos. Ocean. Sci., Vol. 24, No. 3, pp.311-321, June 2013; D. Goodman and Y. Nishimura, "A ground-radar view of Japanese burial mounds", Antiquity 67, pp.349-54.

[2] J.C.F. Wong and R. Shaw, High-level coastal deposits in Hong Kong. GEO Report No.243. Hong Kong: Geotechnical Engineering Office, HKSAR Government, 2009.

[3] Mott Connell, "Agreement No. CE 1/97 remaining development in Tung Chung and Tai Ho comprehensive feasibility study, working paper No. WP12 historical, archaeological & cultural heritage impact assessment", unpublished.

[4] Antiquities and Monuments Office (AMO), "Second territory wide survey of Hong Kong: North Lantau survey", unpublished.

[5] M. Atha, "A military and civilian cemetery of the mid to late Tang maritime trade? Ground penetrating radar (GPR) surveys and excavations at San Tau, North Lantau, Hong Kong", in *Collected Essays of the International Conference on Historical Imprints of Lingnan: Major Archaeological Discoveries of Guangdong, Hong Kong and Macao*, edited by S.L.K. Siu, R.S.K. Yau, J.C.L. Chow, P.S.H. Wong, and Kwok, H-c. Hong Kong, Hong Kong Museum of History, 2014, 176–217.

[6] Cook J.C. Radar transparencies of mine and tunnel rocks, Geophysics 59(2): 202-214, 1975.

[7] W. Meacham (ed.), Sham Wan, Lamma Island: an archaeological site study. Journal Monograph III. Hong Kong: Hong Kong Archaeological Society.